Tautomerism of Sterically Hindered Schiff Bases. Deuterium Isotope Effects on ^{13}C Chemical Shifts

A. Filarowski, A. Koll, M. Rospenk, and I. Krol-Starzomska

Faculty of Chemistry, University of Wroclaw, 14 F. Joliot-Curie Str., 50-383, Wroclaw, Poland

P. E. Hansen*

Department of Life Sciences and Chemistry, Roskilde University, P.O. Box 260, DK-4000 Roskilde, Denmark

Received: November 27, 2004; In Final Form: February 28, 2005

A series of sterically hindered *o*-hydroxy Schiff bases derived from *o*-hydroxyaceto- and benzophenones with very short intramolecular hydrogen bonds were described qualitative and quantitatively by deuterium isotope effects on ^{13}C chemical shift, $^{n}\Delta C(XD)$, $^{n}\Delta F(XD)$, $^{1}J(N,H)$ coupling constants, δNCH_3 chemical shifts and UV spectra. All the investigated compounds are found to be tautomeric. The tautomeric character is described by the signs of the deuterium isotope effects on the ^{13}C chemical shifts. For the 3-nitro-5-chloro derivatives at low temperature, the equilibrium is shifted almost fully toward the proton transferred form in CD_2Cl_2. Intrinsic deuterium isotope effects on chemical shifts of these compounds as well as $^{1}J(N,H)$ coupling constants suggest that a zwitterionic resonance form is dominant for the proton transferred form. Structures, ^{1}H, ^{19}F, and ^{13}C chemical shifts, and deuterium isotope effects on ^{13}C chemical shifts are calculated by ab initio methods. The potential energy functions and the total deuterium isotope effects are calculated, and they are shown to correspond well with the experimental findings.

1. Introduction

Recently Schiff bases have been studied in solution in order to elucidate the proton-transfer mechanism and the position of the equilibrium.[1−18] Schiff bases are interesting as they may serve as simple models for moderately low barrier hydrogen bonding systems[19−21] and because this barrier can be modified in a rather simple manner.[22] Furthermore, the structure (charge separation vs quinoid formation) (Scheme 1) of the proton transferred form has been the subject of investigations for decades.[3,5,6,14,17] Schiff bases play an important role in biological systems and have been investigated intensely as they are believed to play a role in the strengthening of the immune response against cancer and chronic infections diseases including HIV.[23−25] Especially interesting is the finding that Schiff bases with bulky phenyl or naphthyl substituents at the imine group[26,27] are regulators in the central nervous system and act as K^+ channel openers. The most potent was those with a bulky *t*-butoxy group attached to the nitrogen atom. This enabled a steric squeezing between the *t*-butoxy group and the pyridine ring substituted at the imine carbon of the Schiff base.[28] All the Schiff bases mentioned are of the *o*-hydroxy type, which form stable intramolecular hydrogen bonds creating a six-membered pseudo-aromatic ring. The steric aspect is very important as this influences the proton-transfer barrier.

The properties of Schiff bases not least their medical and biological effects relate both to the presence of a tautomeric equilibrium, the position of this equilibrium and to the nature of the tautomeric components. Dudek and Dudek[2,3] pioneered such studies using $^{1}J(N,H)$ coupling constants. Deuterium isotope effects on chemical shifts may be used to describe hydrogen bonded systems both in normal[28] and low barrier hydrogen bonds.[29,30] To push this understanding further we have introduced a combination of studies of deuterium isotope effects on chemical shifts on both ^{13}C and ^{19}F chemical shifts, of carbon−fluorine coupling constants, analysis of selected chemical shifts and combining these measurements with theoretical calculations. Furthermore, UV spectra at variable temperatures may be very useful in establishing the presence of equilibria and providing the equilibrium constants.

The derivatives of *o*-hydroxy acetophenone and *o*-hydroxy benzophenone investigated in this study (Scheme 2) have very short hydrogen bonds with low barriers to proton transfer. Steric effects as caused by the methyl or phenyl groups of the present compounds make the hydrogen bond more linear than for, e.g., Schiff bases of salicylaldehydes.[22]

The aim of the present study is to investigate a large series of compounds with varying steric properties and different substituents including the useful fluorine ones in order to cover a large range of proton-transfer situations and to be able to describe the proton transferred form, called PT.

2. Experimental Section

The following compounds (Scheme 3) were synthesized following a standard procedure[7] (the numbering is given in Scheme 2): 2-(*N*-methyl-α-iminoethyl)-3,5-dibromophenol (**1m**, ×), 2-(*N*-methyl-α-iminoethyl)-3,5-dichlorophenol (**2m**, □), 2-(*N*-propyl-α-iminoethyl)-3,5-dichlorophenol (**2p**, ■), 2-(*N*-methyl-α-iminoethyl)-5-chlorophenol (**3m**, △), 2-(*N*-propyl-α-iminoethyl)-5-chlorophenol (**3p**), 2-(*N*-isopropyl-α-iminoethyl)-3,5-difluorophenol (**4i**), 2-(*N*-methyl-α-iminoethyl)-3,5-difluorophenol (**4m**, ◆), 2-(*N*-isopropyl-α-iminoethyl)-4-fluorophenol (**5i**), 2-(*N*-methyl-α-iminoethyl)-4-fluorophenol (**5m**, ●), 2-(*N*-isopropyl-α-iminoethyl)-5-fluorophenol (**6i**), 2-(*N*-methyl-α-

* To whom correspondence should be addressed. E-mail: POULERIK@ruc.dk. Fax: (+45) 46743011.

10.1021/jp0445977 CCC: $30.25
Published on Web 04/30/2005

SCHEME 1. Tautomeric and Resonance Forms of the Schiff Bases

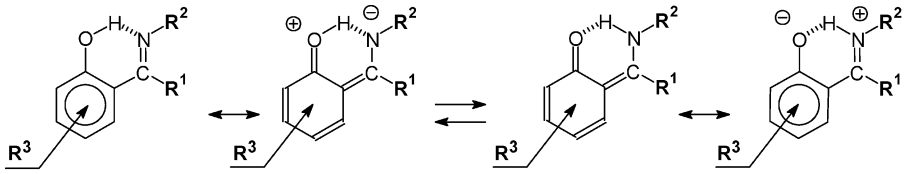

neutral *o*-quinoid keto-enamine zwitterionic

Molecular (M) Form Proton Transfer (PT) Form

SCHEME 2. Numbering

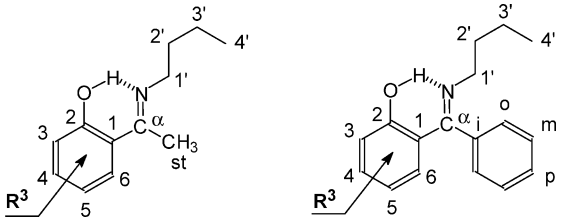

iminoethyl)-5-fluorophenol (**6m**, ○), 2-(*N*-methyl-α-iminoethyl)-phenol (**7m**, ◇), 2-(*N*-ethyl-α-iminoethyl)-4-methyl-5-chlorophenol (**8e**, −), 2-(*N*-methyl-α-iminoethyl)-4-methylphenol (**9m**, ▲), 2-(*N*-methyl-α-iminoethyl)-5-methylphenol (**10m**, +), 2-(*N*-ethyl-α-iminoethyl)-4,5-dimethylphenol (**11e**, ∗), 2-(*N*-methyl-α-iminoethyl)-3-nitro,5-methylphenol (**12m**, ■), 2-(*N*-ethyl-α-iminoethyl)-3-nitro-5-methylophenol (**12e**, ■), 2-(*N*-propyl-α-iminoethyl)-3-nitro-5-methylphenol (**12p**, ■), 2-(*N*-ethyl-α-iminoethyl)-3-nitro-5-chlorophenol (**13e**, •), 2-(*N*-propyl-α-iminoethyl)-3-nitro-5-chlorophenol (**13p**, •), 2-(*N*-methyl-α-iminophenyl)-4-methyl-5-chlorophenol (**14**, ▲), 2-(*N*-methyl-α-iminophenyl)-phenol (**15**, ◆), 2-(*N*-methyl-α-iminophenyl)-4-methylphenol (**16**, ■), 2-(*N*-isopropyl-α-iminophenyl)phenol (**17**), and 2-(*N*-benzyl-α-iminophenyl)phenol (**18**). The **1m**, **4m**, **12m,** and **13m** compounds were ^{15}N enriched using methylammonium chloride, ^{15}N (90%). Deuteriation of the Schiff bases was done by refluxing the compounds in a CH_3OD solution for a short time and evaporation of the solvent under reduced pressure.

The ^{1}H and ^{13}C NMR spectra of samples of nondeuterated and deuterated normally were recorded in dichloromethane (CD_2Cl_2) solutions using a Bruker AC 250, Bruker 500 XL, Varian Mercury 300 and Varian 600 Unity Inova spectrometers. Other solvents like chloroform ($CDCl_3$), pyridine-d_5 (C_5D_5N), dimethyl sulfoxide-d_6, acetone-d_6, or tetrahydrofuran-d_8 (THF-d_8) were also used. NMR parameters were as in a previous investigation.[15] Chemical shifts are referenced through the use of the frequency solvent peak and corrected for temperature effects.

UV spectra were recorded on a Cary 1 UV−vis spectrometer with a homemade two-beam cryostat within 300−180 K range

SCHEME 3. Compounds and Signs of Deuterium Isotope Effects on ^{13}C Chemical Shifts[a]

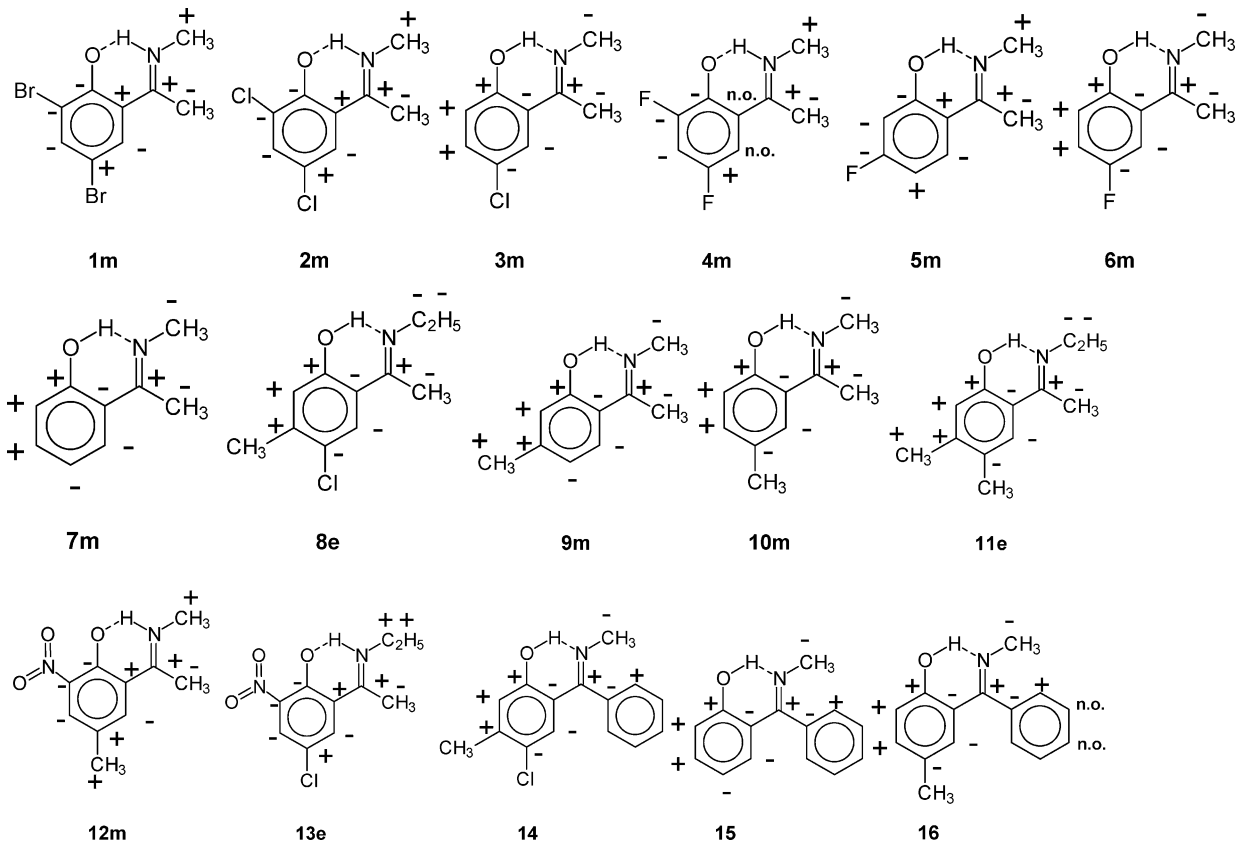

[a] The **m**, **e** and **p** refer to the substituent at N: methyl, ethyl and propyl.

TABLE 1: ^nJ(C,F) Coupling Constants in Hz for 4m, 5m, and 6m

6m	solvent	*T*, K	$J_{C\alpha-F5}$	J_{C1-F3}	J_{C1-F5}	J_{C2-F3}	J_{C2-F5}	J_{C3-F3}	J_{C3-F5}	J_{C4-F3}	J_{C4-F5}	J_{C5-F3}	J_{C5-F5}	J_{C6-F3}	J_{C6-F5}
	CD_2Cl_2	300		3.62	2.92	14.12		233.8	11.42	28.1	22.6	12.0	246.4	2.5	23.7
		220				15.30		231.6	11.95	28.2	22.0	12.7	245.6	3.9	22.9

5m	solvent	*T*, K	$J_{C\alpha-F5}$	J_{C1-F4}	J_{C2-F4}	J_{C3-F4}	J_{C4-F4}	J_{C5-F4}	J_{C6-F4}
	CD_2Cl_2	300			n.o.	19.86	251.78	23.45	12.18
		250		1.65	14.03	18.34	252.73	23.85	12.96
		220			12.54	17.50	253.40	24.04	13.11
		200		1.16	12.96	16.65	253.85	24.13	13.24
		180			14.64	16.05	254.24	24.28	13.60
	THF-d_8	300			13.43	20.75	250.26	23.24	12.22
		290			13.43	21.96	250.26	23.16	12.22
		280			13.35	20.75	249.96	22.86	11.92
		270		1.81	14.03	20.82	250.26	23.24	11.54
		260			14.03	20.14	249.66	23.24	11.62
		250			14.30	20.75	250.26	23.16	12.22
	C_5D_5N	300			14.28	19.72	250.70	23.08	12.04
		250			14.32	19.16	251.05	23.14	12.27
		230			13.94	18.72	251.50	23.16	13.35
	acetone-d_6	250			14.80	19.58	250.22	23.58	12.10
	DMSO-d_6	300			18.04	18.06	250.85	23.69	12.78

4m	solvent	*T*, K	$J_{C\alpha-F5}$	J_{C1-F5}	J_{C2-F5}	J_{C3-F5}	J_{C4-F5}	J_{C5-F5}	J_{C6-F5}
	CD_2Cl_2	220		7.37		7.55	23.07	231.88	23.71
		200	3.09	7.26		7.53	~23	231.92	23.63
		180	2.42	6.92		7.92	21.45	216.06	23.55

TABLE 2: δ(F) Chemical Shift in ppm, $^n\Delta F$(OD) in ppb, and Isotope Effect on Fluorine Chemical Shifts for 4i, 4m, 5i, 5m, 6i, and 6m in CD_2Cl_2

	4i				**4m**			
T, K	δ(F-3)	$^n\Delta$F(OD)	δ(F-5)	$^n\Delta$F(OD)	δ(F-3)	$^n\Delta$F(OD)	δ(F-5)	$^n\Delta$F(OD)
250	−129.0		−134.6	−191.0	−129.3		−134.2	−207.0
220	−129.5	316.0	−134.7	−297.0	−130.2	245.0	−134.2	−322.0
200	−129.8	173.0	−133.8	−378.0	−130.8	389.0	−134.1	−381.0

	5i		**5m**		**6i**		**6m**	
T, K	δ(F-4)	$^n\Delta$F(OD)	δ(F-4)	$^n\Delta$F(OD)	δ(F-5)	$^n\Delta$F(OD)	δ(F-5)	$^n\Delta$F(OD)
250	−106.9	−114.0	−104.9	−93.5	−128.5	−336.0	−126.6	−333.3
230			−104.5	−178.1	−128.7	−369.0		
220	−106.7	−215.0	−104.4	−211.3	−128.9	−392.0	−126.7	−352.2
200	−106.1	−218.0					−126.7	−364.7

in 2 cm quartz cells. The concentrations of approximately 2.8 $\times 10^{-5}$ M solutions were used. The proton-transfer equilibrium constants (K_{PT}) were calculated by: $K_{PT} = C_{PT}/C_M$.[17] The molar absorbance at peak intensity was used to determine the concentration of proton transfer form. The numerical value of this parameter for the PT form was taken from measurements in ethanol. The value was corrected for the dependence of the density of the particular solvent. The absorptions were separated by using the Grams 386 program.[18]

The molecular geometries were optimized using the Gaussian 98 suite of programs[33] and BPW91 Density Functional Theory (DFT) (Beckes exchange[34] and Perdew-Wang correlation term,[35] and a mix of the built in Gaussian type basis sets. The 6-31G** and 6-311++G** basis sets were used. Chemical shifts were calculated using the GIAO approach.[36] Calculations of vibrational levels were performed with the SHOOT program.[37]

3. Results

3.1. Assignments. The assignment of the ^{13}C spectra is not straightforward as the proton transfer makes it difficult to apply substituent effects on chemical shifts. For compounds **4m**−**6m** the carbon fluorine couplings are very useful as the general magnitudes are known. For **4** MBOB[38] spectra have been used to assign the C-3 and C-5 carbons. The assignments of the two-bond couplings at C-4 were done by decoupling experiments. In specific cases deuterium isotope effects due to deuteriation at the CH_3(st) group may be used to assign the α−carbon. The α−carbon may also be assigned by a comparison of methyl, ethyl and propyl derivatives. Having assigned C-α, C-2 can be assigned by default.

For ^{15}N enriched compounds, couplings to ^{15}N are observed at the C-α, C-1′, and C-st carbons and can be used in the assignment of these carbons. ^{13}C chemical shifts are given in Table 1S and those of the ^{1}H chemical shifts in Table 2S.

Signs of deuterium isotope effects on chemical shifts are determined by recording spectra with varied deuterium incorporation at the XH position. Prolonged treatment with methanol-*d* may lead to deuterium incorporation at the CH_3(st) group.

3.2. Deuterium Isotope Effects on ^{13}C Chemical Shifts. The deuterium isotope effects show a very large variation as seen from Table 2S. These variations are indicative of equilibrium isotope effects.[13,16,39−41] Sign patterns are clearly present as seen in Scheme 3. The sign combinations are indicative of the degree of proton transfer. A great deal of correlation is seen from the graphs of Figure 1.

A comparison of the isotope effect data for derivatives with *N*-methyl, ethyl or propyl residues show very similar isotope effects (Table 2S) and hence similar equilibrium constants.

A change of solvent from $CDCl_3$ to CD_2Cl_2 has little effect. An interesting observation is the large change in isotope effects upon change of solvent for, e.g., compounds **5m** and **12m** going from CD_2Cl_2 to THF-d_8.

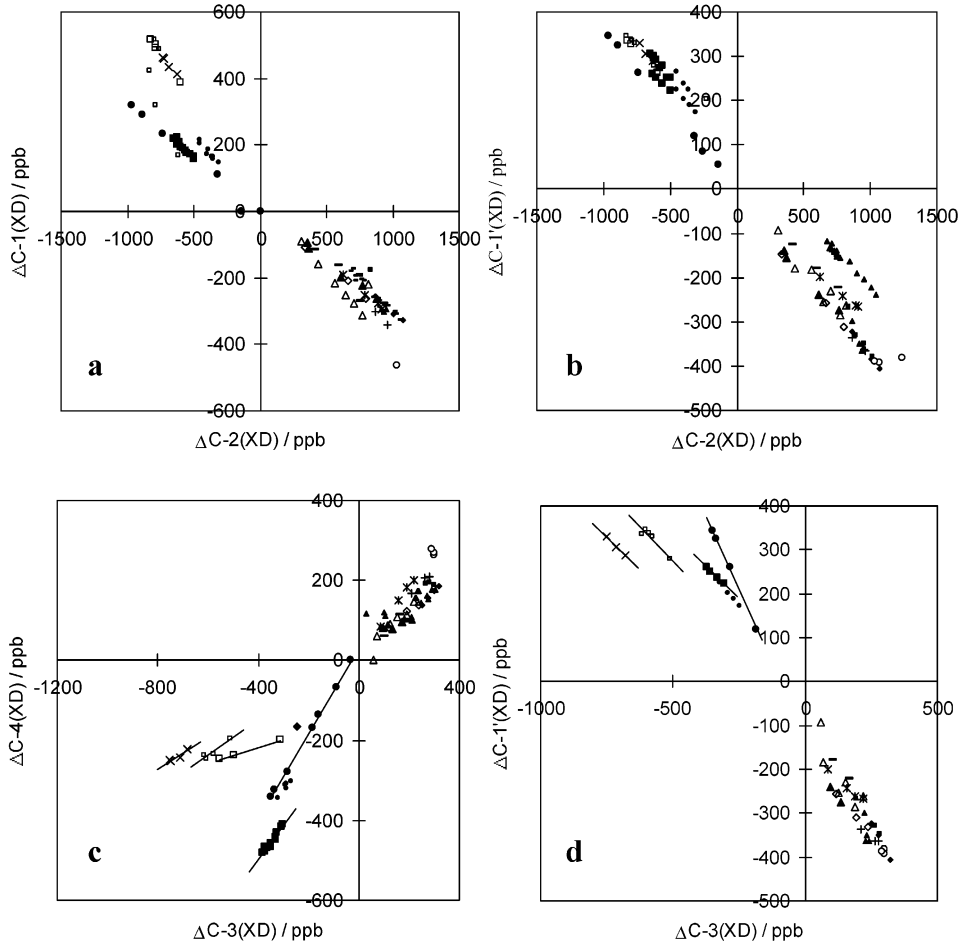

Figure 1. (a) Plots of $^{n}\Delta$C−x(XD) vs $^{2}\Delta$C-2(XD) as well as $^{n}\Delta$C−*x*(XD) vs $^{3}\Delta$C-3(XD). (b) Plot of $^{n}\Delta$C-1′(XD) vs $^{2}\Delta$C-2(XD). (c) Plot of $^{n}\Delta$C-4(OD) vs $^{2}\Delta$C-3(OD). (d) Plot of $^{n}\Delta$C-1′(OD) vs $^{2}\Delta$C-3(OD). The slopes are as follows: **1m**, −0.6; **2m**, −0.6; **5m**, −1.3; **13m**, −0.6. For symbols see Experimental Section.

3.3. ^{19}F Chemical Shifts and Deuterium Isotope Effects on These. The ^{19}F chemical shifts vary according to the substitution pattern (Table 1). Those of high-frequency go at even higher frequency upon lowering of the temperature, whereas the opposite is found for the low-frequency ones. The deuterium isotope effects on ^{19}F chemical shifts are given in Table 2 and are seen to be of both signs. They are very sensitive to changes in the chemical equilibrium as shown previously.[42] The intrinsic effects can be assumed to be small for the fluorine's far from the site of deuteriation as judged from the corresponding *o*-hydroxy ketones,[42] so what is observed is primarily the equilibrium contribution.

3.4. XH Chemical Shifts. It is remarkable that all the XH (OH or NH) chemical shifts have a rather high value and that they are not varying very much, less than 1 ppm (Figure 2a) (Table 2S). The high value is in line with strong hydrogen bonding. The XH chemical shifts fall in two categories, those of compounds with little proton transfer and those with extensive proton transfer. The separation is not so obvious from the chemical shifts but more so from the temperature coefficients. The former group has positive coefficients whereas the latter give slightly negative temperature coefficients (Table 2S) leading to a roughly a parabolic form when plotted vs the mole fraction (derived from ^{1}J(N,H)) (Figure 2). The paraboles are not coinciding due to substituent effects in individual compounds. Plots of δ(XH) vs T^{-1} present linear dependence (δ-(XH) = $-291.85T^{-1} + 18.62$ ($R^2 = 0.9958$)).

3.5. Coupling Constants. ^{1}J(N,H) coupling constants have been measured in a number of selected ^{15}N enriched Schiff bases. ^{1}J(N,H) coupling constants become as large as 93 Hz at low temperature.[4,16] The couplings can be used to estimate the mole fraction of the PT form provided ^{1}J(N,H) of the two tautomers are known. For the molecular form we assume the value of 1.6 Hz given by Kurkovskaya.[4] For the PT-tautomer the situation is more complex. Plots of ^{1}J(N,H) vs T^{-1} for a simple two-component equilibrium like the present are linear.[13] For **13m** in CD_2Cl_2 the value is seen to level off around 80 Hz. The nonlinearity is at high temperature (300−250 K) most likely caused by exchange, whereas at lower temperature the slight nonlinearity is caused by the change in the solvent properties

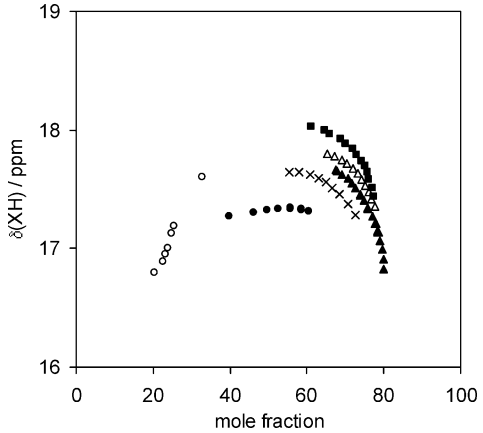

Figure 2. Plot of δXH vs mole fraction: (×) **1m** (CD_2Cl_2); (●) **5m** (CD_2Cl_2); (●) **5m** (THF); (■) **12m** (CD_2Cl_2); (△) **13m** ($CDCl_3$); (▲) **13m** (CD_2Cl_2).

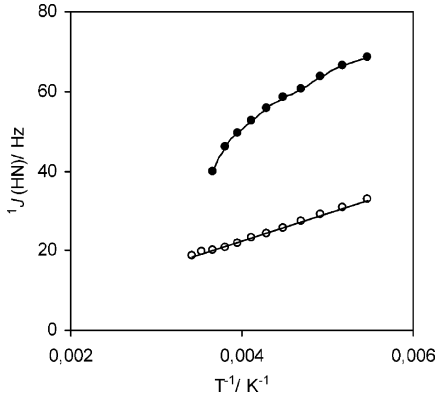

Figure 3. Plot of ^1J(N,H) vs $1/T$: (●) **5m** (CD_2Cl_2); (○) **5m** (THF-d_8) $J(\mathrm{HN}) = 6958.2T^{-1} - 5.335$, $R^2 = 0.9971$.

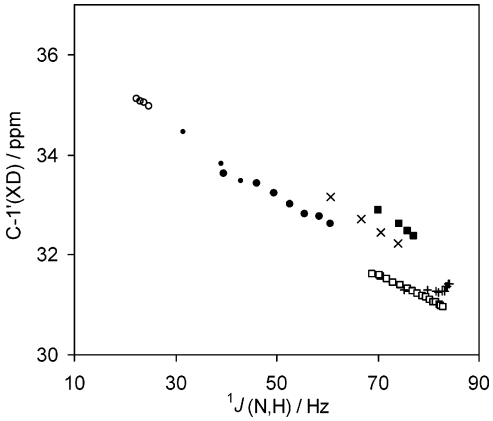

Figure 4. Plot of δC-1′(XD) vs ^1J(N,H): (×) **1m** (CD_2Cl_2); (●) **5m** (CD_2Cl_2); (●) **5m** (C_5D_5N); (○) **5m** (THF); (■) **12m** (CD_2Cl_2), (+) naph. **m** ($CDCl_3$); (□) naph. **m** (CD_2Cl_2).

upon cooling as no such nonlinearity is observed in THF-d_8 (Figure 3). Furthermore, as this is seen for different compounds with different K_{PT} and hence different degrees of proton transfer at different temperatures. This cannot be related to a molecular property. That ^1J(N,H) for nitro derivatives is less than 92.5 Hz (value suggested by Kurkovskaya[4,5]) agrees with the findings of naphthalene derivatives in which it was found that ^1J(N,H) varied to some extent with substituents.[16] A value of 80 Hz is therefore used as the one describing the fully proton transferred form of nitro derivatives.

Another interesting type of coupling constant is the carbon−fluorine one, ^nJ(C,F), found in compounds **4m**−**6m** (Table 2). The ^1J(C-5,F) coupling constant for **6m** is smaller than seen in fluorobenzene, whereas for **4m** the one-bond coupling of C-3 is similar to that of fluorobenzene.[43] These couplings are markedly smaller than that found in **5m**. The ^1J(C,F) coupling constants are in general less for **5m** in acetone-d_6, DMSO-d_6, THF-d_8 and C_5D_5N than in CD_2Cl_2. The ^1J(C,F) coupling constant for **5m** in CD_2Cl_2 is seen to increase significantly when the temperature is lowered. The temperature effects of the measured coupling values are much less pronounced in pyridine. For **4m** and **6m** only a slight increase with temperature is found. Differences in two two-bond couplings ^2J(C-3,F) and ^2J(C-5,F) for **5m** are seen.

3.6. δC-1′(δNCH_3). As small ^1J(N,H) couplings are difficult to measure because of exchange it is hence difficult to use this parameter to measure mole fractions in the entire range and δC-1′ has been tested as a possible measure of the degree of proton transfer. This group is sitting in a similar type of environment in all *N*-methyl derivatives and will clearly respond to proton transfer. Theoretical calculations suggest that the values for the M form is fairly constant for different types of compounds and the same is found for the PT form (see later). A plot of δC-1′ vs ^1J(N,H) couplings shows linear correlations for single compounds in specific solvents (Figure 4). A plot of two-bond isotope effects vs δNCH_3 or vs ^1J(N,H) show the well-known S-shaped graph indicative of a tautomeric equilibrium[39] (Figures 5a and 5b). The PT form has the smallest C-1′ chemical shifts. Similar plots can of course also be done for δNCH_2CH_3 and δN$CH_2CH_2CH_3$.

3.7. Theoretical Calculations. Geometries have been optimized for both the M and PT forms in the B3LYP DFT functional using a 6-31G** basis set. The theoretical calculations

TABLE 3: Calculated ^{13}C Chemical Shift Differences and Deuterium Isotope Effects on Chemical Shifts

compound		C-α	C-1	C-2	C-3	C-4	C-5	C-6	C-1′	Cst	F-3	F-4	F-5
2m	slope[a] M form	−11.0	13.9	−29.1	−9.0[h]	−5.7	11.3	0.3	9.7	0.3			
	slope[a] PT form	−28.9	5.5	9.3	13.5	0.3	1.0[h]	0.8	−10.9	−1.9			
5m	slope[a] M form	−9.7	11.3	−31.7	−6.9[h]	−4.1	7.1	−0.8	9.6	0.0			
	slope[a] PT form	−30.1	7.3	10.0	8.9[h]	3.1	4.2	0.5	−10.4	−1.6			
7m	slope[a] M form	−10.3	13.1	−30.8	−8.7[h]	−5.5	9.0	0.0	8.9	0.0			
	slope[a] PT form	−29.9	7.6	10.7[h]	8.9[h]	−0.2[h]	3.2	1.4	−9.9	−1.0[h]			
	estimated intrinsic isotope effect[b]	0.12	−0.16	0.37	0.10	0.06	−0.11	0.00	−0.11	0.00			
	estimated intrinsic isotope effect[b]	1.31	−0.33	−0.47	−0.39	0.01	−0.14	−0.06	0.44	0.04			
	estimated intrinsic isotope effect[c]	−0.44	−0.18	0.29	0.05	0.05	−0.12	−0.01	−0.05	0.00			
	estimated equilibrium isotope effect[d]	−0.20	−0.15	0.49	0.28	0.11	−0.13	−0.01	−0.26	−0.05			
	estimated isotope effect[e]	0.23	−0.32	0.78	0.33	0.16	−0.25	−0.02	−0.31	−0.05			
	measured isotope effect[f]	0.44	∼−0.3[f]	0.80	0.19	0.12	−0.28	−0.10	−0.31	−0.09			
2m	$\sigma C_M - \sigma C_{PT}$[i]	−6.1	−4.2	11.5	8.2	2.3	−3.9	−0.3	−6.9	−1.1			
4m		−6.0	−6.3	16.5	7.0	2.4	−5.3	−2.7	−6.6	−1.3	6.3		−4.1
5m		−5.0	−2.9	12.2	4.4	3.1	−0.4	−0.5	−6.6	−1.3		2.9	
6m		−5.8	−5.6	14.7	8.1	5.9	−2.8	−2.5	−6.8	−1.3			−3.9
7m		−5.3	−4.1	13.1	7.6	2.9	−3.4	−0.3	−6.8	−1.4			
12m		−4.3	−2.9	10.3	4.6	4.8	−4.8	−0.4	−6.2	−1.1			
13m		−3.2	−3.1	9.4	4.8	4.7	−4.7	0.6	−6.1	−1.1			

[a] The slope, dσ/dr, is obtained from a plot of ^{13}C chemical shifts vs the N−H bond lengths. [b] The intrinsic isotope effects are obtained by multiplying the slope with the change in the XH bond length upon deuteriation (see text). [c] The estimated intrinsic isotope effects are a weighted average of the intrinsic effects for the M and PT forms. [d] The equilibrium isotope effects are obtained by multiplying the difference in nuclear shieldings ($\sigma C_M - \sigma C_{PT}$) as taken from Table 3 with the difference in zero point energies of the H- and D forms. [e] The estimated isotope effects are the sum of the equilibrium and the intrinsic isotope effects. [f] The isotope effects are measured at ambient temperature. [g] The slopes are not fully linear in this range. [h] Estimated value as the isotope effect could not be measured at ambient temperature, but only at a slightly lower temperature (see Table 2S). [i] Nuclear shieldings obtained from ab initio calculations.

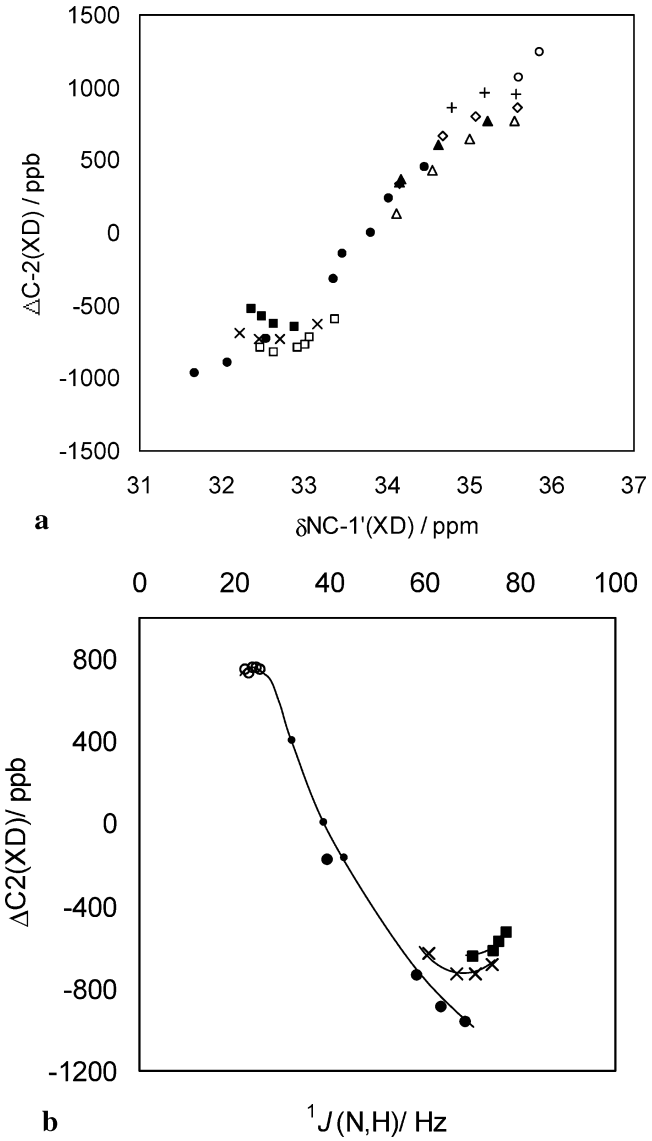

Figure 5. (a) Plot of $^2\Delta$C-2 (XD) vs δC-1′: (×) **1m**; (□) **2m**; (△) **3m**; (●) **5m**; (○) **6m**; (◇) **7m**; (▲) **9m**; (+) **10m**; (■) **12m**. b). Plot of $^2\Delta$C-2(OD) vs ^1J(N,H): (×) **1m** (CD_2Cl_2); (●) **5m** (CD_2Cl_2); (•) **5m** (C_5D_5N); (○) **5m** (THF-d_8); (■) **12m** (CD_2Cl_2).

show a clear-cut although moderate variation in the series **2m**−**7m** and **12m**. $R_{O\cdots N(M)}$, $R_{O\cdots N(PT)}$, $R_{OH(M)}$ and $R_{NH(PT)}$ are as follows: **2m** (2.521, 2.503, 1.020, 1.064 Å), **3m** (2.540, 2.498, 1.013, 1.070 Å), **4m** (2.542, 2.511, 1.013, 1.061 Å), **5m** (2.534, 2.500, 1.016, 1.069 Å), **6m** (2.545, 2.496, 1.011, 1.069 Å), **7m** (2.542, 2.491, 1.012, 1.073 Å), **12m** (2.508, 2.494, 1.025, 1.065 Å), and **13m** (2.504, 2.494, 1.027, 1.065 Å). An important and characteristic feature is the rather short OH bond considering the short N···O distances. In addition, potential functions in two dimensions have been traced by varying the X−H distances in the adiabatic (Figure 6, parts a and b) approach using the basis set 6-31G** for **2** and **5**, and 6-311++G** for **7** (see also ref 44). It should be noted that solvent effects are not included in these calculations. Such work is in progress in general, but is not likely to lead to different isotope effects as these are insensitive to solvent effects.[45]

^{1}H and ^{13}C chemical shifts have been calculated for both the M and PT forms in the ab initio B3LYP GIAO approach[36] of compounds **2m**, **4m**−**7m**, **12m**, and **13m**. It is important to notice that the ^{1}H chemical shieldings transform into chemical shifts that resemble the experimental ones at ambient temperature. The ^{13}C chemical shift differences are given in Table 3, and the chemical shifts differences for one carbon do not vary very much from compound to compound (Table 3).

In addition, XH chemical shifts changes as a function of the XH bond length have been calculated. These $\delta\sigma/dr_{NH}$ values (referred to as slope) are used as a basis for evaluation of the intrinsic isotope effects in the M and PT forms.[29] Figure 7 exemplifies this for C-α. The slopes for compounds **2m**, **5m**, and **7m** are seen to be quite similar (Table 3). The change in the bond length upon deuteriation, $\Delta R_{XH(D)}$, is calculated using the SHOOT program.[37] $\Delta R_{XH(D)}$ was obtained by averaging over all vibrational levels below the barrier. However, this made no difference in this case as the higher vibrational levels were populated scarcely in contrast to recent reports for picolinic *N*-oxide[30a] and hydrogen phthalate.[30b] From the M form a $\Delta R_{OH(D)}$ of 0.012 Å for **7m** and 0.016 Å for **2m** is found. For the PT form we found $\Delta R_{NH(D)} = 0.044$ Å for **7m**. Multiplying the slopes obtained from plots of ^{13}C chemical shifts vs N−H bond length with the $\Delta R_{XH(D)}$ values give estimates of intrinsic isotope effects.[29] Slopes are listed in Table 3. The actual intrinsic isotope effects are a weighted average (see Table 3). The equilibrium isotope contributions are obtained by multiplying the difference in nuclear shieldings for the M and PT forms (Table 3) with the change in the mole fraction upon deuteriation, ΔX_D. The latter value is calculated from the difference in zero point energies for the M and PT forms of the H and D species, respectively. For **7m**, the zero point energies for the M and PT forms are 14.69 and 12.38 kJ for the H forms and 9.73 and 10.71 kJ for the D forms, giving a difference of 9.96 kJ in favor of the M form. The equilibrium constant for **7m** has been determined by UV measurements to be close to 11% PT form in CD_2Cl_2 (Tables 3S and 4S). Using this values the change in the mole fraction upon deuteriation is 0.0375.

Isotope effects of particular interest are those of $^2\Delta$C-2(OD), $^4\Delta$C-α(OD), $^2\Delta$C-α(ND) and $^4\Delta$C-2(ND). The calculated intrinsic isotope effects for the M form are seen to inter-depend (Table 3) in a fashion similar to what has been found experimentally for the corresponding hydrogen bonded ketones and aldehydes.[46] For the PT form a large $^2\Delta$C-α(ND) is predicted, which dominates the total isotope effect. For C-3 and C-1′ the equilibrium isotope contribution dominates according to calculations (Table 3).

The XH proton shieldings show rather steep slopes when plotted toward the OH or the NH distance, but also as seen previously[29] that the correlations are rather linear (Figure 7).

3.8. UV Spectra. UV spectra have been recorded at variable temperature in different solvents, CH_2Cl_2 (Figure 8 and Table 2S) and THF (Table 2S). The UV data for **5m**, **12m**, and **13m** (Table 3S) show slightly higher percentages of PT form than seen from the NMR measurements based on ^1J(N,H) coupling constants. This is especially true for the two latter in CD_2Cl_2.

4. Discussion

The key parameters determining the properties of Schiff bases are the position of the tautomeric equilibrium and the properties of the two tautomeric forms. Those of the molecular form (Scheme 1) can easily be obtained from nontautomeric compounds. Those of the PT form are much more elusive. Ways to measure the position of the proton-transfer equilibrium are ^1J(N,H), the $^2\Delta$C(XD) isotope effect and also to a certain extent δC-1′(δNCH$_3$) as demonstrated in the results section. A third approach is to measure UV spectra at variable temperature that enables a description of the two states and a determination of the equilibrium constant.

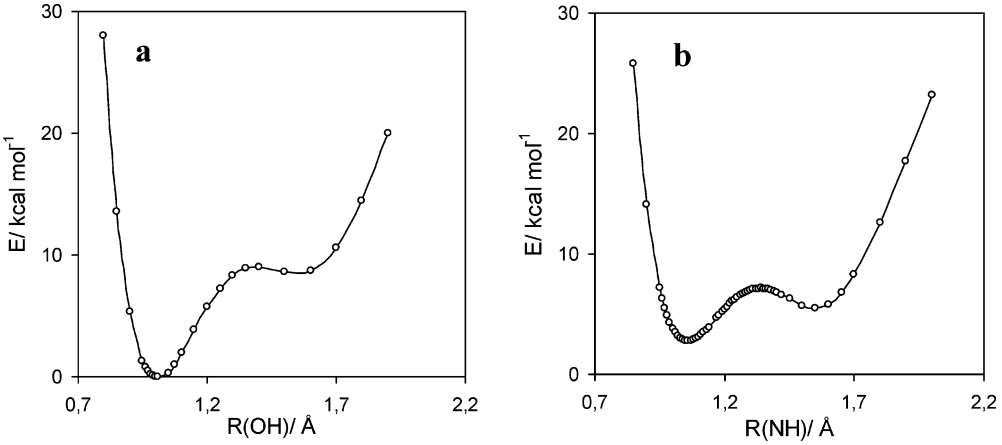

Figure 6. Potential curves for the M and the PT form (**7m**).

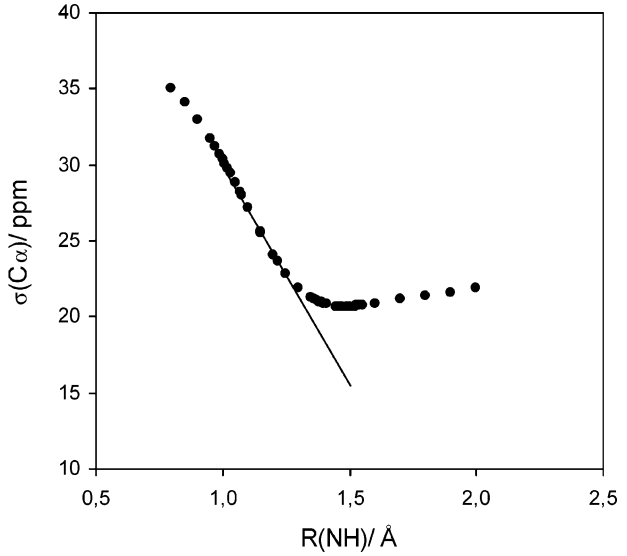

Figure 7. Plot of calculated σ(Cα) vs NH bond lengths (**7m**) σ(Cα) $= -28.815R(\mathrm{NH}) + 58.687$).

4.1. Deuterium Isotope Effects on ^{13}C Chemical Shifts. The isotope effects on chemical shifts are in a simple model as the present composed of two contributions, the intrinsic and the equilibrium one.[39] The former cannot be observed directly in the present compounds as they are all take part in an equilibrium (see later). From studies of the corresponding ketones, it is known that the intrinsic isotope effects scale with hydrogen bond strength.[47] They can therefore be expected to be rather large. The intrinsic part is of course a weighted average of the values of the two tautomers. The equilibrium part depends on the chemical shift difference between carbons of the two tautomers multiplied by the change in the mole fraction upon deuteriation.[39] The graphs of Figure 1 must be seen in this light. As the chemical shift differences for different compounds are slightly different, slightly different slopes are obtained as seen from Figure 1, parts c and d. However, as the chemical shift difference is not very solvent dependent values for different solvents are expected to fall on the same line. As seen from the graphs of Figure 1 do most of the isotope effects correlate rather well (this is also the case for isotope effects not shown). The majority of the few outliers are due to compounds that show an usually large two-bond isotope effect (see Figure 5) and to a minor extent substituted carbons, e.g., C-5 of the 3,5-dichloro derivative, etc. Two exceptions are the isotope effects of C-α and C-st. In the former case one group of compounds are clearly different, those with phenyl substitutents at C-α (**14**−**18**). In the latter case the intrinsic contribution is apparently dominating giving an intrinsic effect in the M form of −100 ppb, a value to be compared with a similar enamine.[46,48]

Plots of the $^2\Delta$C(XD) isotope effects vs δC-1′ or ^1J(N,H) are seen to have the S-shape characteristic for an equilibrium system (Figure 5, parts a and b). Combined with the sign combinations of isotope effects (Schemes 3 and 4), the XH proton chemical shift and the temperature coefficients of the chemical shift of the XH proton ($\delta(\mathrm{XH}) = -291.85T^{-1} + 18.62$) this gives a unique way of determining the mole fraction. On the basis of the parameters the equilibrium constants fall in the following order: **18**, **16**, **17**, **15**, **14**, **11e**, **7m**, **3m**, **3p**, **9m**, **8e**, **4m**, **5m**, **1m**, **2m**, **2p**, **12m**, **12e**, **12p**, and **13e**, **13p**. It is very evident that the nitro group in the 3-position enhances the proton transfer.

As seen from Figure 5, parts a and b, the maxima have different amplitudes. This was also found for naphthalene derivatives.[16] This can be understood based on the differences in ^{13}C chemical shifts of carbons of the two tautomers as seen in Table 3 and from the finding that the intrinsic isotope effects at C-2, $^2\Delta C(XD)_{int}$, can be quite large in nitro substituted cases as judged from *o*-hydroxy acetyl derivatives.[49]

The isotope effects observed in **13e** and **13p** at 180 K resemble each other and are also close to those of **12m**, **12e**, and **12p** and give the approximate values for the intrinsic effects of the PT form, as the compounds are close to 100% at the PT form and no or very little equilibrium isotope effects contribute. The relatively large intrinsic isotope effects observed far from the site of deuteriation tell about an extensively delocalized system. The small magnitude of $^2\Delta$C-α(XD) is remarkable compared to values in ketoenamines.[46,48] The small value derived for **12** and **13** can thus be seen to be a consequence of mesomeric forms. This is confirmed as ^1J(N,H) couplings in nitro derivatives are smaller than in the other derivatives, which can be taken as evidence for the zwitterionic form being dominant (see Scheme 5).

4.2. ^nJ(C,F). For **5m**, having a substituent in 4-position, the one bond coupling constant is larger than that found in *p*-hydroxyfluorobenzene and the coupling constant is increasing with lowering of the temperature in CD_2Cl_2. This is easily understood from the resonance structures of Scheme 5, because the one-bond carbon−fluorine coupling increases with the bond order.[50] Such an effect can best be obtained from the zwitterionic resonance forms (PTB and PTC), whereas the quinone form (PTD) does not allow the fluorine to be mesomerically involved. The temperature dependence shows that the PT form is contributing more and more as the temperature is lowered. The

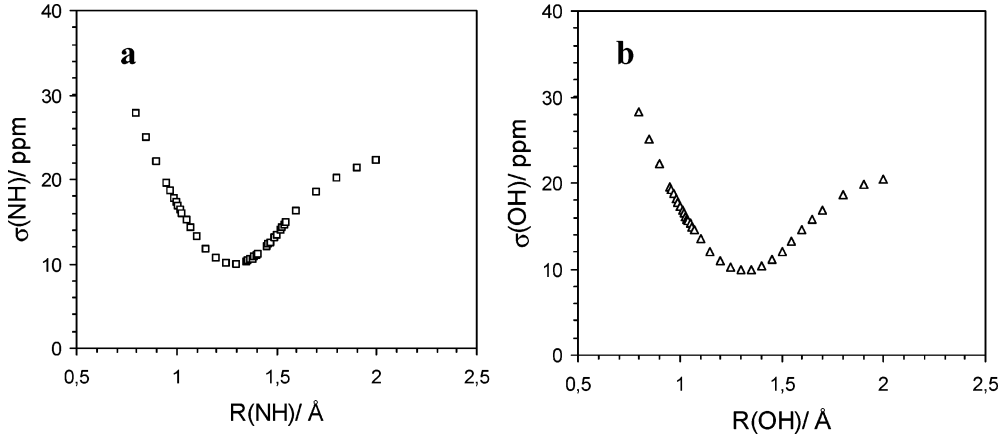

Figure 8. Plot of calculated σNH vs OH or NH bond lengths (**7m**).

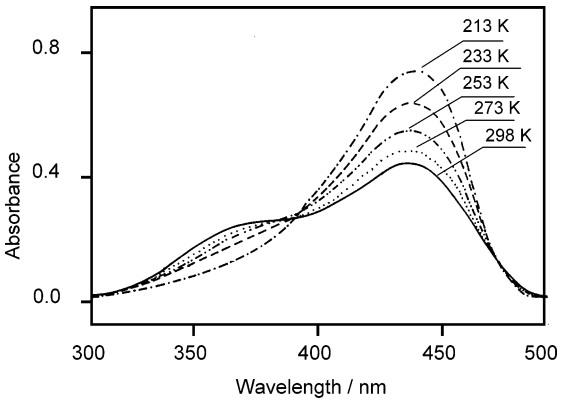

Figure 9. UV spectra of **13m**. Variable temperature in CH_2Cl_2.

SCHEME 4. Typical Sign Patterns of Deuterium Isotope Effects on ^{13}C Chemical Shifts

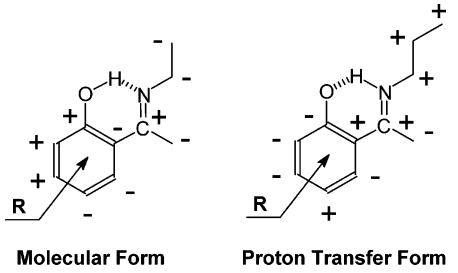

finding that for **4m** ^1J(C-3,F) and for **6m** ^1J(C-5,F) are less than those observed in fluorobenzene[50] but similar to that in *p*-hydroxyfluorobenzene suggests that the fluorine is not involved in stabilization as seen from the resonance structures of Scheme 5.

Not only the one-bond but also the two-bond,^2J(C,F), coupling constant depends on bond order, but for the two bond coupling in such a way that the lower the bond order the larger the coupling constant.[50] For **5m** ^2J(C-3,F) < ^2J(C-5,F), which clearly shows that the resonance forms like PTA or PTD of Scheme 5 contribute to the structure.

4.3. ^{19}F Chemical Shifts. Compared to the ^{19}F chemical shift of *p*-fluorophenol (−126.5 ppm)[51] the chemical shift of **5m** is seen to be at higher frequency whereas that of **6m** is almost unchanged and those of **4m** to lower frequency with that of F-3 the most. Furthermore, the finding that these tendencies are amplified at lower supports the mesomeric schemes discussed above (see also Scheme 5).

4.4. δC-1′. As the chemical shifts show a linear dependence with ^1J(N,H) (Figure 4) they clearly reflect the change in the

SCHEME 5. Resonance Forms of 3-Nitro- and 4-Fluoro Derivatives of Schiff Bases Such as 12, 13, and 5

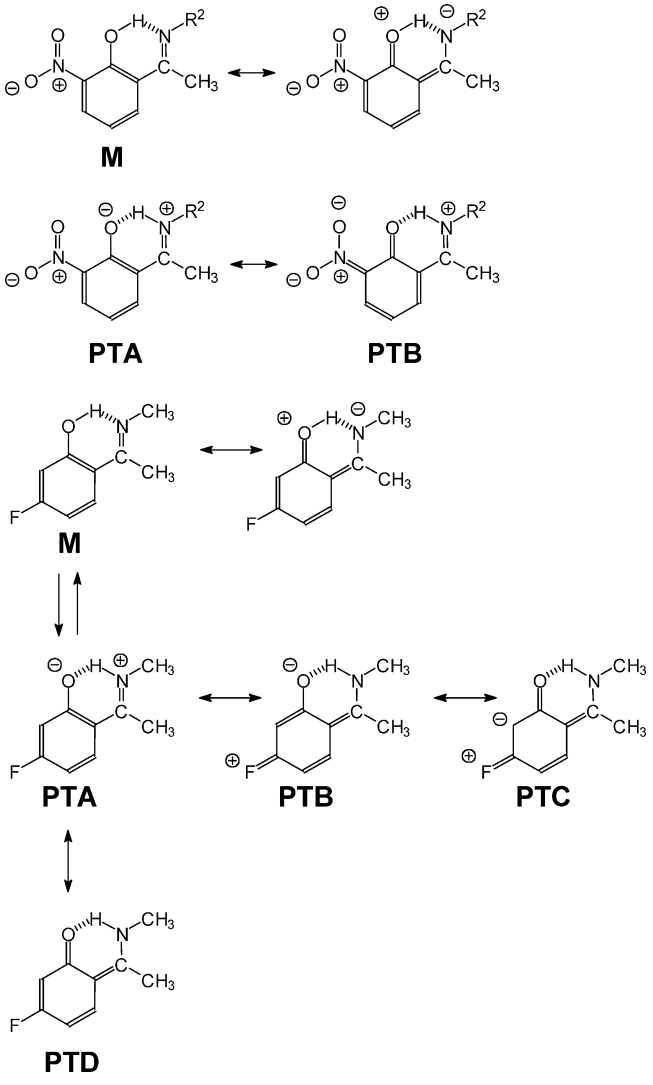

equilibrium constant. However, as the chemical shift difference between the M form and the PT form is moderate, ~6 ppm and as the δC-1′ seems to depend on both the type of compound and the solvent (Figure 4) the mole fraction obtained will only be qualitative. On the other hand, the finding that compounds like **1m**, **5m**, and **12m** fall on different lines in CD_2Cl_2 indicates that the C-1′ chemical shift reflect something else in addition to the degree of proton transfer. An indication is seen from the

Schiff base of 1-hydroxy-2-acenaphthone. In $CDCl_3$ the value increases as the temperature is lowered associated with a more polar solvent. The explanation could thus be that the charge separated PT form (A) is increased at lower temperature and in more polar solvents. This would also explain the order **5m** > **1m** > **12m** (see discussion on ^1J(C,F) of **5m** and ^1J(N,H) of nitro derivatives).

4.5. Theoretical Calculations. Potential curves have been calculated using either an adiabatic approach or a full relaxation method both cases applying the B3LYP approach and the 6-31G** basis set. Both approaches led to very low barriers for the PT form and to long N−H bonds. Using these geometries calculated ^{1}XH chemical shifts are unrealistic. An improvement for **7** is obtained by applying a basis set of the type 6-311++G** (Figure 6). This led to a higher interconversion barrier, which again led to a shorter and more well-defined N−H bond length and a XH chemical shift in agreement with observation.

The characterization of a hydrogen bonded system is typically done by the parameters $R_{O\cdots N}$ and R_{OH} and R_{NH}. These are seen from the calculations to vary somewhat. For **2m**, **5m**, **7m**, and **12m**, the $R_{O\cdots N}$ length is decreasing for the M form, whereas the variation of the PT form is marginal. The variation of the former is in line with the tendency to proton transfer.

A question of much interest is obviously for a low barrier system like the present how the hydrogen bond behaves and how proton transfer is taking place. A central player is the XH proton. This can be monitored directly via the ^{1}H chemical shift or indirectly via the secondary isotope effects on carbon chemical shifts. The NH protons for all the compounds fall at low field and the variation between compounds is small. The latter feature supports the calculation of bond length showing that these do not vary very much from compound to compound. As the slope of the nuclear shielding for the XH proton is steep (Figure 8), this would lead to a large difference in NH chemical shifts if bond lengths varied much and this as seen above has not been found. Furthermore, the variation with mole fraction is also very moderate indeed (Figure 2). However, as the slope is linear (Figure 8) this does not exclude large symmetrical bond length fluctuations from the mean bond length. Another possibility would be that the N−H bond lengths were close to 1.3 Å, but the calculations are not supporting this at all and the derived NH chemical shifts for such a situation do not correspond to the observed chemical shifts.

5. Conclusions

The combined results from NMR and UV measurements reveal clearly that all compounds are tautomeric. The strong hydrogen bond present, as seen from the very large XH chemical shifts, promote proton transfer as compared with the corresponding Schiff bases derived from substituted salicylaldehydes. The compounds with phenyl substituents (**14**−**18**) show smaller equilibrium constants than their corresponding alkyl derivatives (**1**−**13**). The substituents on the phenol ring clearly plays an important role. Judging from the deuterium isotope effects, the ^1J(N,H) coupling constants and the UV spectra the equilibrium constant can be ranked with increasing equilibrium constants in the following order: **18**, **16**, **17**, **15**, **14**, **11e**, **7m**, **3m**, **3p**, **9m**, **8e**, **4m**, **5m**, **2m**, **3m**, **1m**, **12m**, **12e**, **12p**, and **13e**, **13p**. For the 3-nitro derivatives **13e** and **13p** full proton transfer is taking place at low temperature. The isotope sign patterns clearly indicate the type, either M form or PT form. For these compounds the temperature behavior of ^1J(N,H) as well as the chemical shift behavior of C-1′ and $^2\Delta$C(XD) show that a zwitterionic resonance form contributes significantly to the PT form. For the 4-fluoro derivative ^nJ(C,F) couplings demonstrate that for the PT form the mesomeric forms with no charge on nitrogen contribute strongly.

Solvents such as CD_2Cl_2 promote proton transfer as compared to pyridine and tetrahydrofuran.

For this relatively low barrier system a potential can be derived, which gives realistic NMR chemical shifts parameters. In addition, both the intrinsic and the equilibrium part of the isotope effects on chemical shifts can be calculated leading to a reasonable prediction of the total isotope effect on chemical shifts.

Acknowledgment. The authors wish to thank Dr. Wei Zhang and Anne Lise Gudmundsson for help with recording spectra. A.F. thanks the Danish Natural Science Research Council for providing a postdoctoral fellowship and support for our H-bond research. The authors also wish to thank J. Mavri and J. Stare for providing a copy of the SHOOT program and B.V. Hansen for his help.

Supporting Information Available: Tables of ^{13}C chemical shifts, deuterium isotope effects on ^{13}C chemical shifts and XH chemical shifts, thermodynamic characteristics of proton-transfer equilibria, and proton-transfer equilibrium constants. This material is available free of charge via the Internet at http://pubs.acs.org.

References and Notes

(1) Metzler, C. M.; Cahill, A.; Metzler, D. E. *J. Am. Chem. Soc.* **1980**, *102*, 6075.
(2) Dudek, G.; Dudek, E. P. *J. Chem. Soc. B* **1971**, 1356.
(3) Dudek, G.; Pitcher-Dudek, E. *J. Am. Chem. Soc.* **1966**, *88*, 2407.
(4) Kurkovskaya, L. N. *Zh. Strukt. Khim.* **1977**, *19*, 946.
(5) Kurkovskaya, L. N.; Nurmukhametov, R. N.; Shygorin, D. N. *Zh. Strukt. Khim.* **1980**, *21*, 61.
(6) Sitkowski, J.; Stefaniak, L.; Dziembowska, T.; Grech, E.; Jagodzinska, E.; Webb, G. A. *J. Mol. Struct.* **1996**, *381*, 177.
(7) Alarcon, S. H.; Olivieri, A. C.; Gonzalez-Sierra, M. *J. Chem. Soc., Perkin Trans. 2* **1994**, 1067.
(8) Salman, S. R.; Lindon, J. C.; Farrant, R. D. *Magn. Reson. Chem.* **1993**, *31*, 991.
(9) Vargas V. C. *J. Phys. Chem.* **2004**, *108*, 281. Hadjoudis, E. *Mol. Eng.* **1995**, *5*, 301.
(10) Hadjoudis, E. *Mol. Eng.* **1995**, *5*, 301.
(11) Ohshima, A.; Momotake, A.; Arai, T. *J. Photochem. Photobiol. A* **2004**, *162*, 473.
(12) Katritzky, A. R.; Ghiviriga, I.; Leeming, P.; Soti, F. *Magn. Reson. Chem.* **1996**, *34*, 518.
(13) Hansen, P. E.; Sitkowski, J.; Stefaniak, L.; Rozwadowski, Z.; Dziembowska, T. *Ber. Bunsen-Ges. Phys. Chem.* **1998**, *102*, 410.
(14) Rozwadowski, Z.; Dziembowska, T. *Magn. Reson. Chem.* **1999**, *37*, 274.
(15) Rozwadowski, Z.; Majewski, E.; Dziembowska, T.; Hansen, P. E. *J. Chem. Soc., Perkin Trans. 2* **1999**, 2809.
(16) Dziembowska, T.; Rozwadowski, Z.; Filarowski, A.; Hansen, P. E. *Magn. Reson. Chem.* **2001**, *39*, S67.
(17) (a) Krol-Starzomska, I.; Rospenk, M.; Rozwadowski, Z.; Dziembowska, T. *Pol. J. Chem.* **2000**, *74*, 1441. (b) Rospenk, M.; Krol-Starzomska, I.; Filarowski, A.; Koll, A. *Chem. Phys.* **2003**, *287*, 113.
(18) GRAMS/386. Galactic Industries Corporation, New Hampshire, USA.
(19) (a) Cleland, W. W.; Kreevoy, M. M. *Science* **1994**, *264*, 1887. (b) Warshel, A.; Papazyan, A.; Kollman, P. A. *Science* **1994**, 102.
(20) Frey, R. A.; Whitt, S. A.; Tobin, J. B. *Science* **1994**, *264*, 1927.
(21) Madsen, G. K. H.; Iversen, B. B.; Larsen, F. K.; Kapon, M.; Reisener, G. M.; Herbstein, F. H. *J. Am. Chem. Soc.* **1998**, *120*, 10040.
(22) (a) Filarowski, A.; Glowiak, T.; Koll, A. *J. Mol. Struct.* **1999**, *484*, 75. (b) Filarowski, A.; Koll, A.; Glowiak, T. *Monatsh. Chem.* **1999**, *130*, 1097. (c) Filarowski, A.; Koll, A.; Glowiak, T. *J. Chem. Soc., Perkin Trans. 2* **2002**, 835. (d) Filarowski, A.; Koll, A.; Glowiak, T. *J. Mol. Struct.* **2002**, *615*, 97.
(23) Zheng, B.; Brett, S.; Tite, J. P.; Brodie, T. A.; Rhodes, J. *Science* **1992**, *256*, 1560.
(24) Hui, M. B. V.; Lien, E. J.; Trousdale, M. D. *Antiviral Res.* **1994**, *24*, 261.

(25) Koneru, P. B.; Lien, E. J.; Avramis, V. I. *Pharm. Res.* **1993**, *10*, 515.

(26) Kaplan, J.-P.; Raizon, B. M.; Desarmenien, M.; Feltz, P.; Headley, P. M.; Worms, P.; Lloyd, K. G.; Bartholini, G. *J. Med. Chem.* **1980**, *23*, 702.

(27) Krause, M.; Rouleau, A.; Stark, H.; Luger, P.; Lipp, R.; Garbarg, M.; Schwartz, J.-C.; Schunack, W. *J. Med. Chem.* **1995**, *38*, 4070.

(28) Maekawa, T.; Yamamoto, S.; Igata, Y.; Ikeda, S.; Watanabe, T.; Shiraishi, M. *Chem. Pharm. Bull.* **1997**, *45*, 1994.

(29) Abildgaard, J.; Bolvig, S.; Hansen, P. E. *J. Am. Chem. Soc.* **1998**, *120*, 9063.

(30) (a) Stare, J.; Jezierska, A.; Ambrozic, G.; Kosir, I. J.; Kidric, J.; Koll, A.; Mavri, J.; Hadzi, D. *J. Am. Chem. Soc.* **2004**, *126*, 4437. (b) Westler, W. M.; Weinhold, F.; Markley, J. L. *J. Am. Chem. Soc.* **2002**, *124*, 14373.

(31) Harris, T. K.; Mildvan, A. S. *Proteins* **1999**, *35*, 275.

(32) Furnuss, B. S.; Hannaford, A. J.; Smith, P. W.; Tatchell, A. *Vogel's Textbook of Practical Organic Chemistry*; Longman: New York, 1989, p 997.

(33) Gaussian98 (Revision A.7), Frisch, M. J.; Trucks, G. W.; Schlegel, H. B.; Scuseria, G. E.; Robb, M. A.; Cheeseman, J. R.; Zakrzewski, V. G.; Montgomery, J. A.; Burant, J. C.; Dapprich, S.; Millam, J. M.; Daniels, A. D.; Kudin, K. N.; Strain, M. C.; Farkas, O.; Tomasi, J.; Barone, V.; Cossi, M.; Cammi, R.; Mennucci, B.; Pomelli, C.; Adamo, C.; Clifford, S.; Ochterski, J.; Petersson, G. A.; Ayala, Y.; Cui, Q.; Morokuma, K.; Malick, D. K.; Rabuck, A. D.; Raghavachari, K.; Foresman, J. B.; Cioslowski, J.; Ortiz, J. V.; Stefanov, B. B.; Lui, G.; Liashenko, A.; Piskorz, P.; Komaromi, I.; Gomperts, R.; Martin, R. L.; Fox, D. J.; Keith, T.; Al-Laham, M. A.; Peng, C. Y.; Nanayakkara, A.; Gonzalez, C.; Challacombe, M.; Gill, P. M. W.; Johnson, B. G.; Chen, W.; Wong, M. W.; Andres, J. L.; Head-Gordon, M.; Replogle, E. S.; Pople, J. A. Gaussian, Inc.: Pittsburgh, PA, 1998.

(34) (a) Becke, A. D. *J. Chem. Phys.* **1992**, *96*, 2155. (b) Becke, A. D. *J. Chem. Phys.* **1992**, *97*, 9173. (c) Becke, A. D. *J. Chem. Phys.* **1993**, *98*, 5648.

(35) Lee, C.; Yang, W.; Parr, R. G. *Phys. Rev. B* **1988**, *37*, 785.

(36) Ditchfield, R. *Mol. Phys.* **1974**, *27*, 789.

(37) Stare, J.; Mavri, J. *Comput. Phys. Commun.* **2002**, *143*, 222.

(38) Meissner, A.; Sørensen, O. W. *Magn. Reson. Chem.* **2000**, *38*, 981.

(39) Bolvig, S.; Hansen, P. E. *Magn. Reson. Chem.* **1996**, *34*, 467.

(40) Hansen, P. E. in *Isotope Effects on Chemical Shifts as a Tool in Structural Studies*; Jensen, H. T., Ed.; Roskilde University Press: Roskilde, Denmark, 1996.

(41) Bolvig, S.; Hansen, P. E. *Curr. Org. Chem.* **2000**, *4*, 19.

(42) Hansen, P. E.; Bolvig, S.; Buvari-Barcza, A.; Lycka, A. *Acta Chem. Scand.* **1997**, *51*, 881.

(43) Weigert, F. J.; Roberts, J. D. *J. Am. Chem. Soc.* **1971**, *93*, 2361.

(44) Filarowski, A.; Koll, A.; Hansen, P. E. *J. Phys. Chem.* **2005**, in preparation.

(45) Hansen, P. E. *Annu. Rep. NMR* **1983**, *15*, 106.

(46) Zheglova, D. Kh.; Genov, D. G.; Bolvig, S.; Hansen, P. E. *Acta Chem. Scand.* **1997**, *51*, 1016.

(47) Hansen, P. E. *Magn. Reson. Chem.* **1992**, *31*, 23.

(48) Hansen, P. E.; Kawecki, R.; Krowczynski, A.; Kozerski, L. *Acta Chem. Scand.* **1990**, *44*, 826.

(49) West-Nielsen, M.; Dominak, P. M.; Wozniak, K.; Hansen, P. E. *J. Phys Org. Chem.* To be submitted.

(50) Hansen, P. E.; Berg, A.; Jakobsen, H. J.; Manzara, A. P.; Michl, J. *Org. Magn. Reson.* **1977**, *10*, 179.

(51) Bradamante, S.; Pagani, G. A. *J. Org. Chem.* **1980**, *45*, 114.